

## 6.6.2 Differential Mass Balance (DMB)

The Differential Mass Balance (DMB) model, as described in Appendix 6C, was applied to ambient concentrations measured at Hopi Point in Grand Canyon National Park and at Page, Arizona in the Glen Canyon National Recreation Area. The DMB model is a receptor model, combined with elements of a deterministic model, which is designed to calculate the fraction of an ambient concentration contributed by one or more sources of interest (in this case NGS). The DMB model was applied to ambient  $SO_4$  and  $SO_2$  data at Hopi Point as well as at Page.

As noted in Appendix 6C, the fundamental DMB equation involves the scaling of ambient tracer concentrations by the ratio of emissions of the species of interest (in this case  $SO_2$ , the parent species for  $SO_4$ ) to tracer, multiplied by a factor that accounts for the deposition and chemical conversion (i.e., oxidation) of sulfur species during the time required for the plume parcel to be transported to the measurement site. Thus, the DMB model calculations are based on the NGS plume ages derived in Section 6.4.3 and estimates of the rates of deposition and conversion. The reported DMB calculations were carried out using those deposition and conversion rates that were most consistent with the observed data from among the ranges of values supported by a literature review. The following two sections summarize the results of this review.

### Choice of Deposition and Oxidation Rates in the DMB Model.

Since the literature review of deposition rates supported quite a wide range of possible deposition rates (i.e., deposition velocities for  $SO_2$  ranging from 0.1 to 2.3  $cm/s$  and 0 to 0.9 for sulfate), this full range of deposition rates was tested in all possible combinations in the DMB model. In addition sulfur oxidation rates were varied such that:

$$k_c = C * (RH/100\%) \text{ where } 0 < C < 4 \text{ percent per hour.} \quad (6.6)$$

Clearly, not all combinations of the  $SO_2$  and sulfate  $v_d$ 's and the conversion rate would yield physically reasonable results. Thus, the DMB model was optimized by selecting combinations of deposition parameters that explained the most variance in the measured sulfate data at Hopi Point.

The optimization was carried out by exercising the DMB model (see Appendix 6C) for all combinations of the following three parameters:

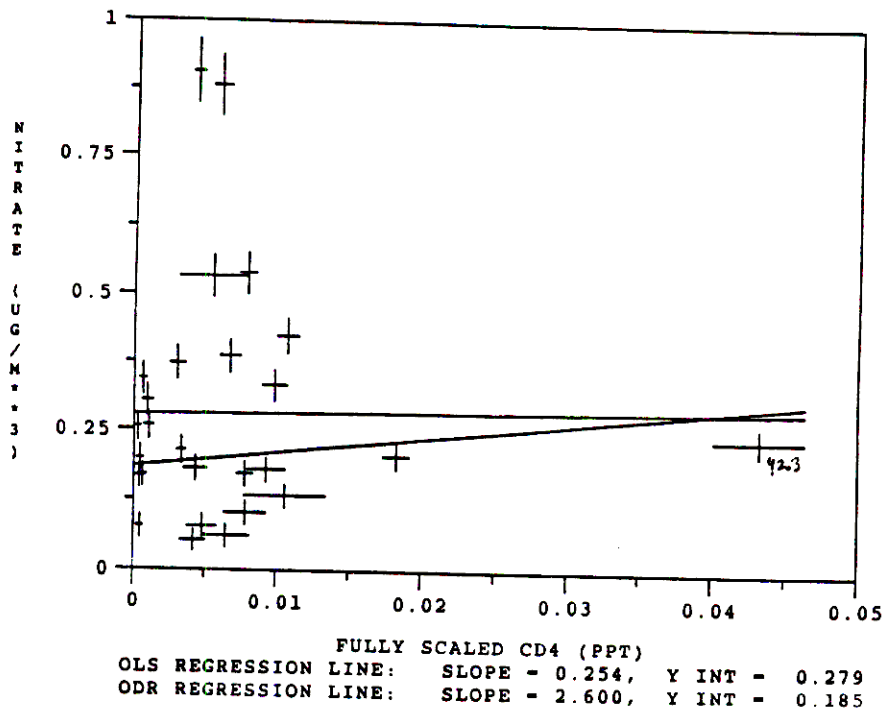
Deposition rate for  $SO_2$ :  $v_1 = 0.1$  to  $2.3 \text{ cm/s}$  in increments of  $0.1 \text{ cm/s}$  (23 values).

Deposition rate for sulfate:  $v_2 = 0.0$  to  $0.9 \text{ cm/s}$  in increments of  $0.05 \text{ cm/s}$  (19 values).

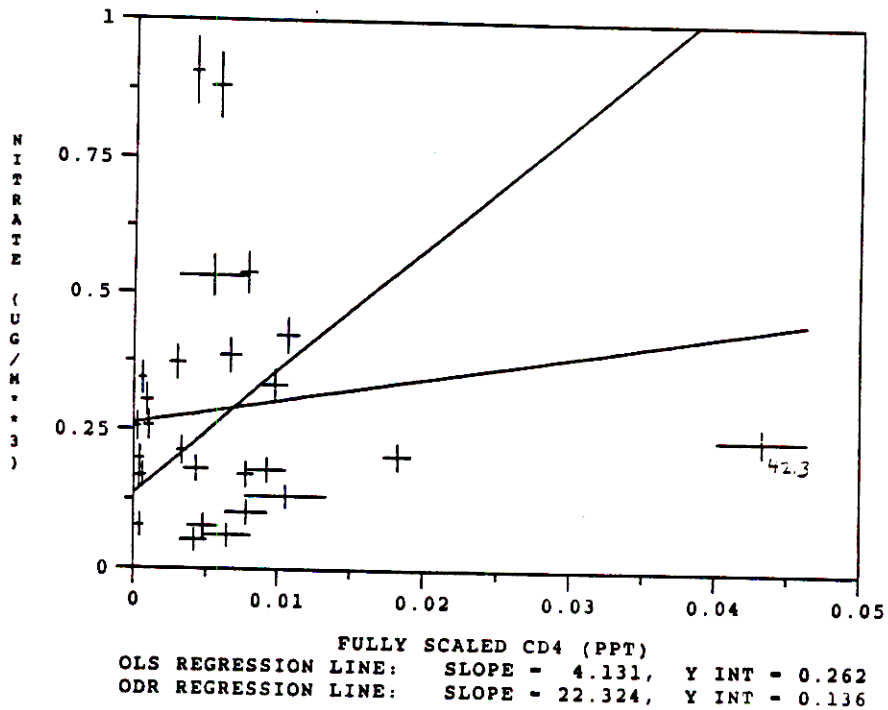
$SO_2$  Conversion (at 100% RH):  $C = 0.0$  to  $4.0 \text{ \%}/h$  in increments of  $0.5 \text{ \%}/h$  (9 values).

Thus, a total of 3,933 different combinations of these three fundamental parameters ( $23 \times 19 \times 9$ ) were used in separate DMB calculations for each 12-hour period of data for Hopi Point. The deposition velocities were used in combination with an assumed mixing height ( $H_m$ ) of 700 meters. This height was based on the sum of the average measured NGS plume centerline height of 600 meters and expected vertical mixing of 100 meters over distances of approximately 100  $km$  (e.g., the Pasquill-Gifford  $\sigma_z$  at  $x = 100 \text{ km}$  for F stability is 90 meters). The NGS plume age used in these calculations was the maximum of either 12 hours or the youngest age from Table 6.10. The total ambient sulfate concentration  $C_{SO_4,k}$  for each time period  $k$  must satisfy an equation of the form:

$$C_{SO_4,k} = \beta_0 + C_{SO_4,NGS,k} + \beta_{As} C_{As,k} \quad (6.7)$$

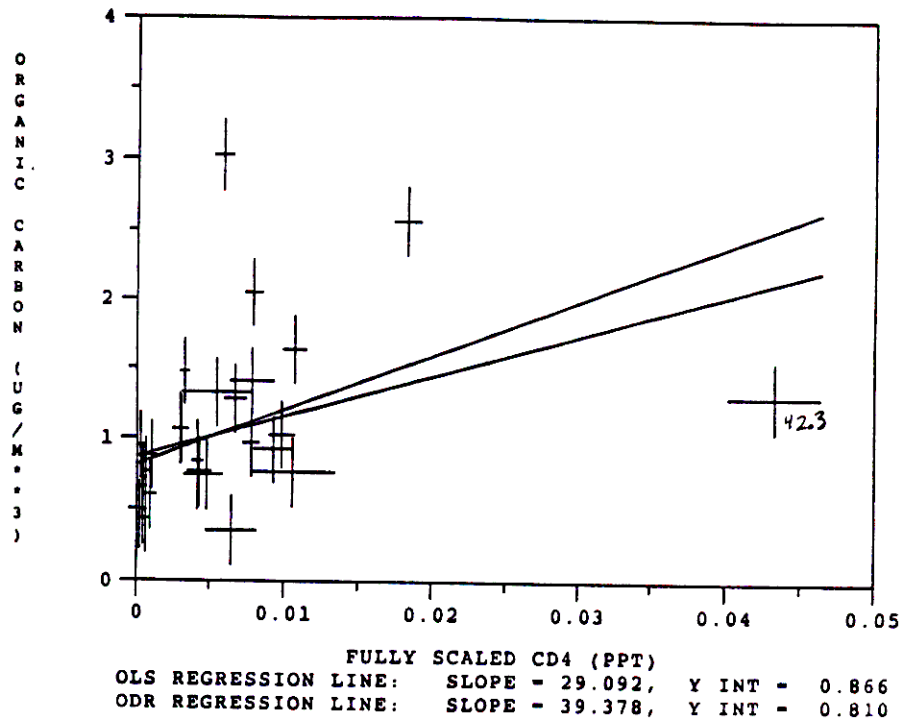


a) With day 42.3 in regressions.

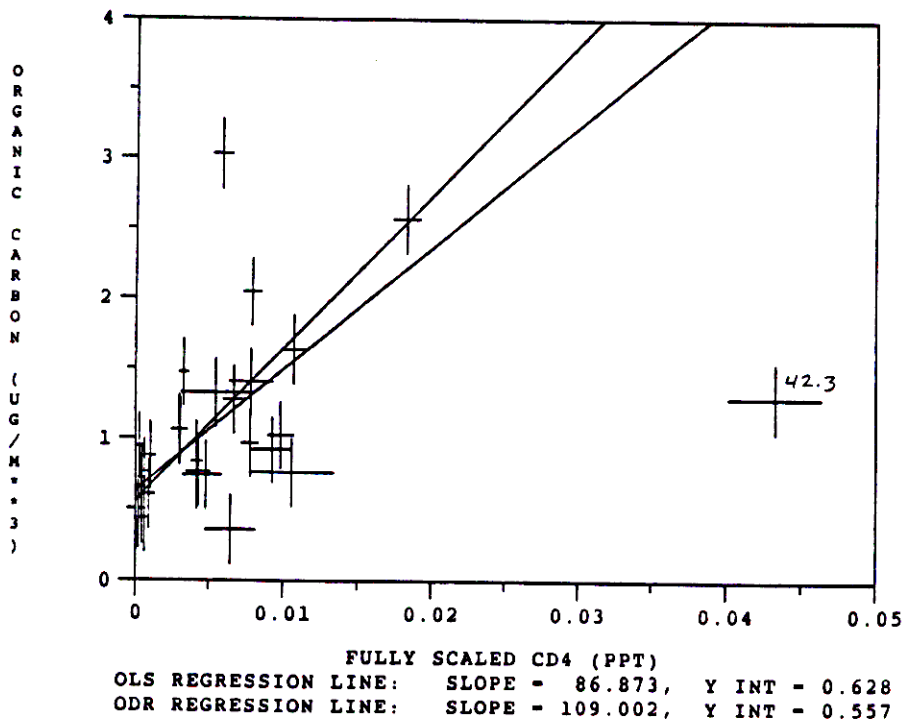


b) Without day 42.3 in regressions.

Figure 6.55: Scatter plot of  $SCD_4$  vs particulate nitrate at Page along with the OLS and ODR regression lines.

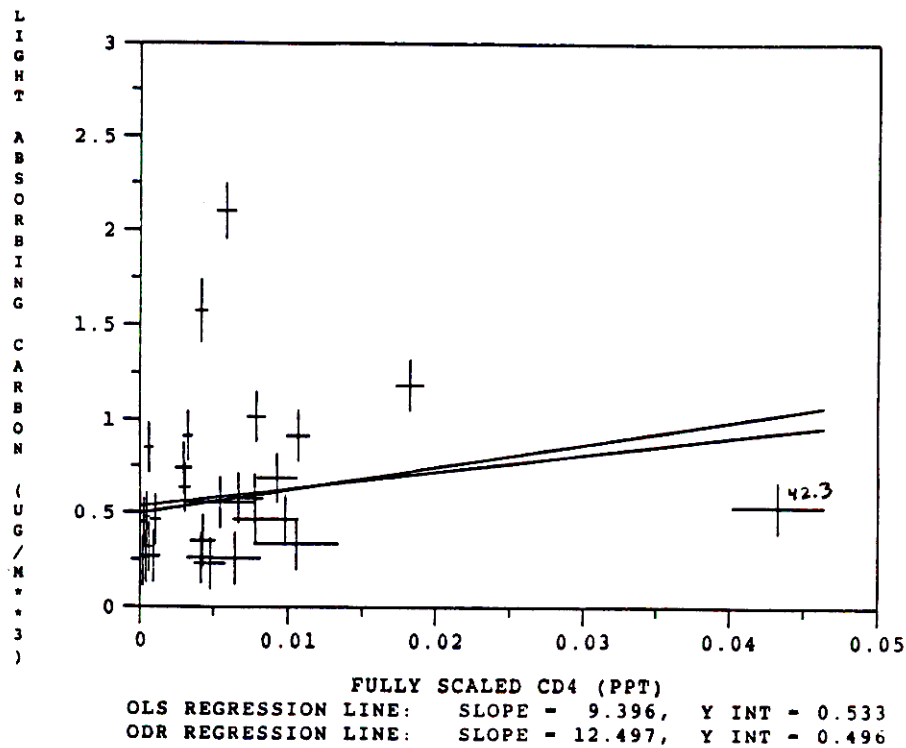


a) With day 42.3 in regressions.

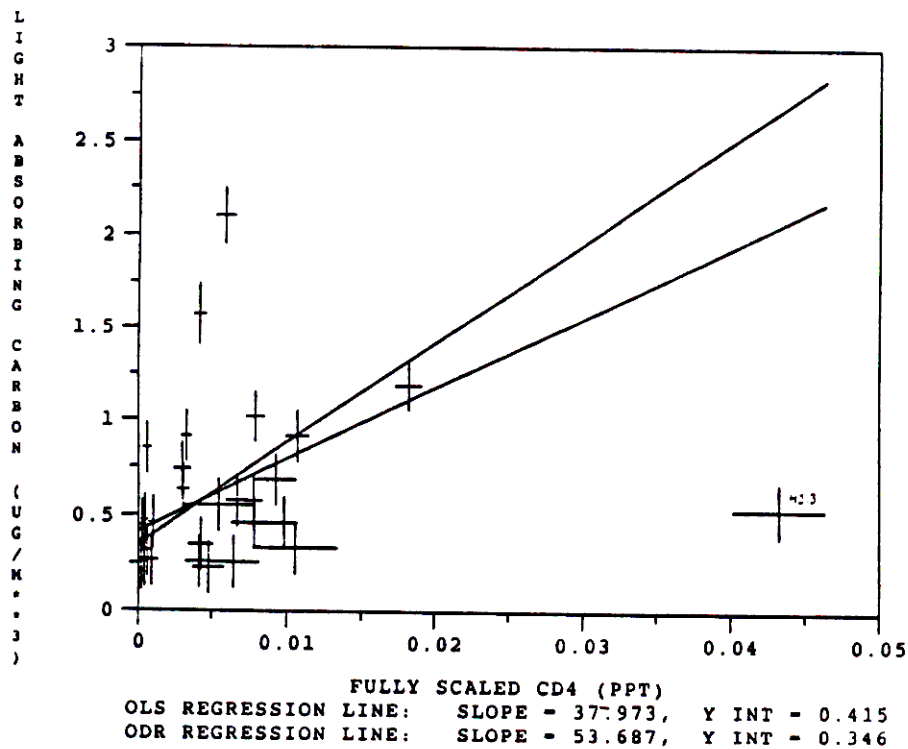


b) Without day 42.3 in regressions.

Figure 6.56: Scatter plot of  $SCD_4$  vs organic carbon at Page along with the OLS and ODR regression lines.



a) With day 42.3 in regressions.



b) Without day 42.3 in regressions.

Figure 6.57: Scatter plot of  $SCD_4$  vs light absorbing carbon at Page along with the OLS and ODR regression lines.

as shown in the TMBR section and Appendix 6B. All combinations of deposition velocities for  $SO_2$  and sulfate and  $C$  were identified such that the regression fit resulted in an  $R^2$  of 0.70 or greater. Out of the 3,933 combinations of parameters tested, 407 combinations were found to provide an  $R^2$  greater than 0.70. The DMB calculations using this smaller set of parameter values was assumed to represent the range of plausible NGS contributions.

Figure 6.58 (a through e) shows the combinations of deposition velocities and oxidation rates with  $R^2 > 0.70$ . Isopleths for  $R^2 = 0.70, 0.73,$  and  $0.75$  are presented. These figures indicate that many different combinations of deposition velocities and oxidation rates yield reasonably high  $R^2$  values. However, higher  $SO_2$  deposition velocities are combined with lower sulfate deposition velocities, and vice versa.

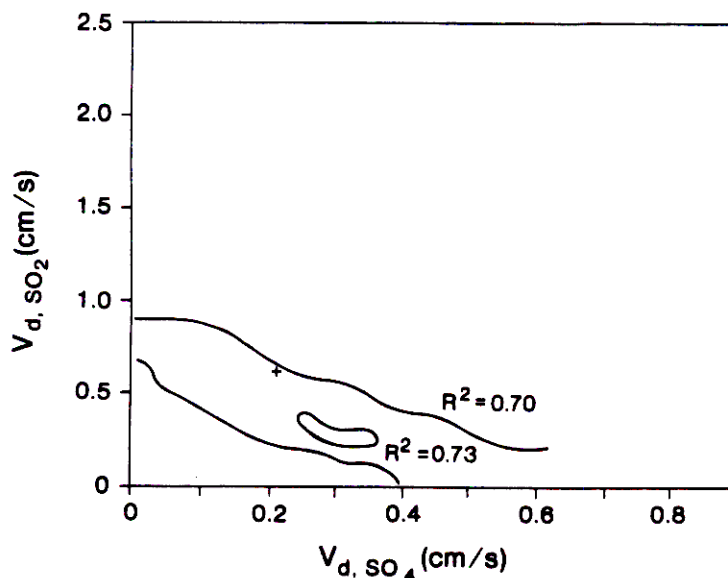


Figure 6.58: a. Combinations of deposition velocities for  $SO_2$  and sulfate and  $SO_2$  oxidation rates having  $R^2 > 0.70$ .  $k_c = 1.0\%/h \times RH/100$ .

The highest  $R^2$  (0.77) was achieved with deposition velocities for  $SO_2$  and sulfate of 0.91 and 0.14  $cm/s$  and a oxidation rate ( $C$ ) of .017 times RH 1/hour. The empirically optimum deposition rates are consistent with the median of the literature deposition velocities, 0.70 and 0.20  $cm/s$ , respectively.

#### Application of the DMB Model with Optimized Parameters

This optimum set of deposition and conversion parameters produced an average NGS contribution to sulfate at Hopi Point over the WHITEX time period of 68 percent. Figure 6.59 shows the computed average NGS fraction of total sulfate at Hopi Point for all 407 combinations of deposition velocities and oxidation rates producing  $R^2 > 0.70$ . Although the average NGS fraction of total sulfate is 0.68 for the combination of parameters that gives the highest  $R^2$  ( $= 0.77$ ), the NGS fraction of total sulfate ranges from 0.43 to 0.96 for all combinations of parameters with  $R^2 > 0.70$ . Thus, NGS on average is calculated to contribute  $68 \pm 28$  percent of the ambient sulfate measured at Hopi Point during the WHITEX period.

Table 6.41 and Figure 6.60 (a and b) show the time history of the total sulfate, the NGS sulfate, and the NGS fraction of total ambient sulfate during the WHITEX period. The table

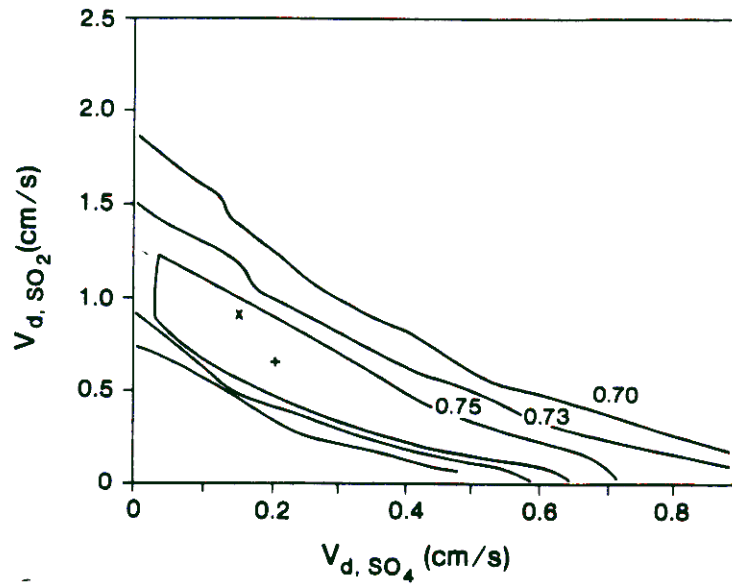


Figure 6.58: b. Combinations of deposition velocities for  $SO_2$  and sulfate and  $SO_2$  oxidation rates having  $R^2 > 0.70$ .  $k_c = 1.5\%/h \times RH/100$ .

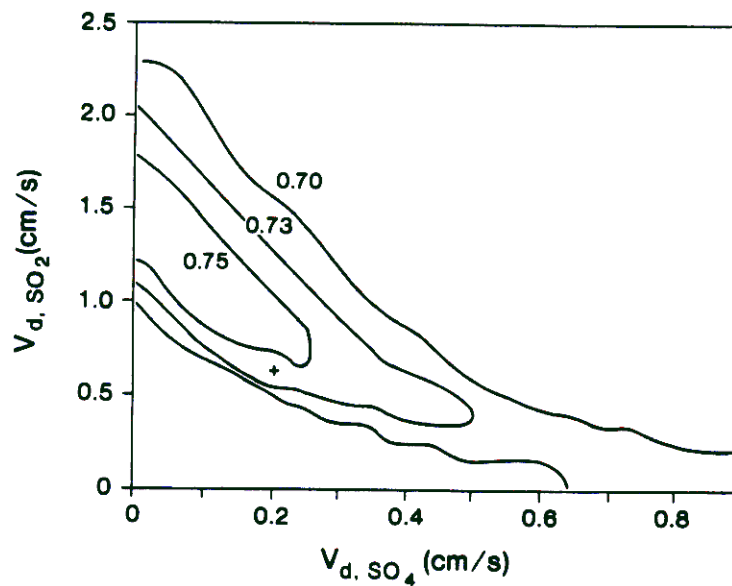


Figure 6.58: c. Combinations of deposition velocities for  $SO_2$  and sulfate and  $SO_2$  oxidation rates having  $R^2 > 0.70$ .  $k_c = 2.0\%/h \times RH/100$ .

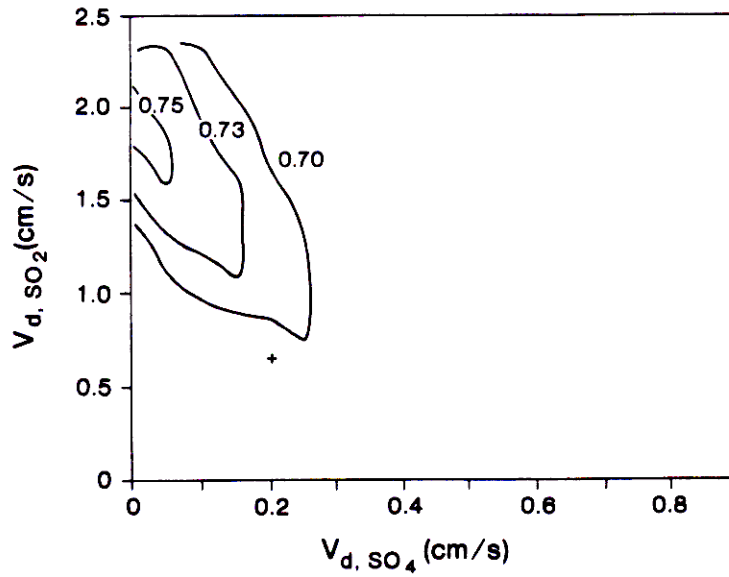


Figure 6.58: d. Combinations of deposition velocities for  $SO_2$  and sulfate and  $SO_2$  oxidation rates having  $R^2 > 0.70$ .  $k_c = 2.5\%/h \times RH/100$ .

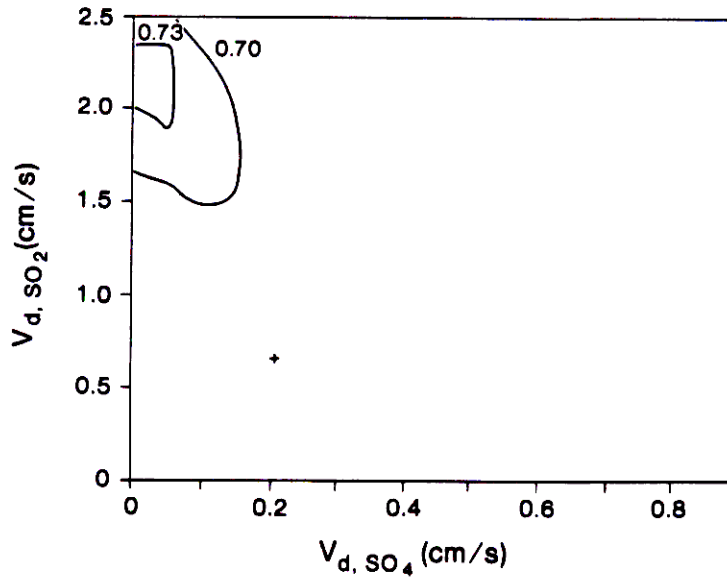


Figure 6.58: e. Combinations of deposition velocities for  $SO_2$  and sulfate and  $SO_2$  oxidation rates having  $R^2 > 0.70$ .  $k_c = 3.0\%/h \times RH/100$ .

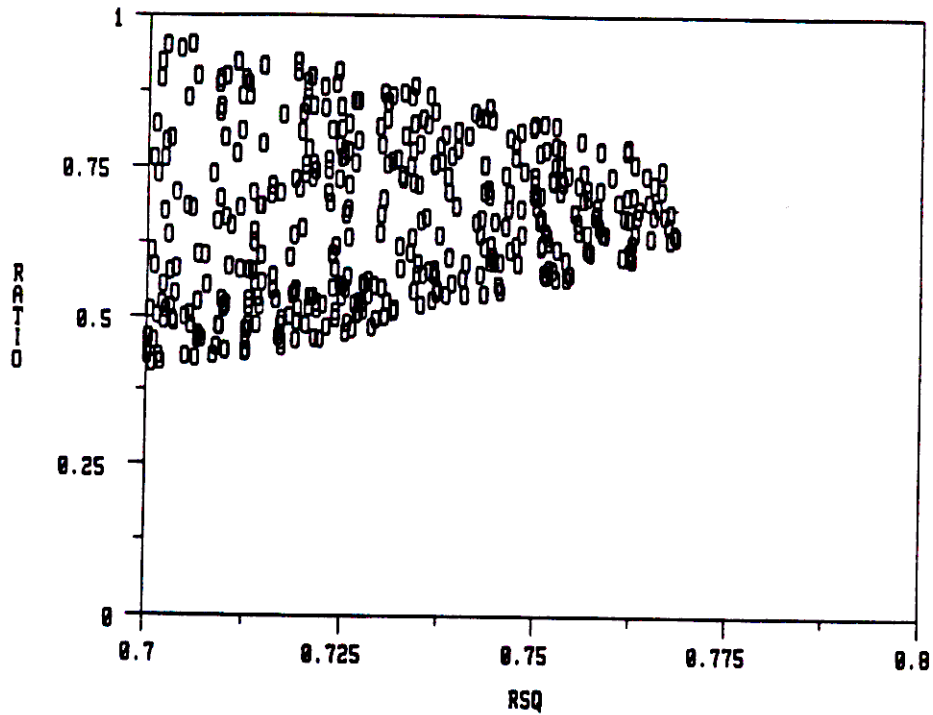


Figure 6.59: Calculated average NGS fraction of total ambient sulfate at Hopi Point for all combinations of  $SO_2$  and sulfate deposition velocities and oxidation rates yielding  $R^2 > 0.70$ .

shows uncertainties associated with (1) the range of deposition velocities and oxidation rates that yield  $R^2 > 0.70$  and (2) the measurement uncertainties (including the uncertainty in plume age, judged to be + 20 percent). Since the two categories of uncertainty are expected to be independent, the total uncertainty (standard error) is calculated from the square root of the sum of the squares:

$$E_{total} = (E_k^2 + E_m^2)^{1/2}. \quad (6.8)$$

Figure 6.60 (a) shows the best estimate of the NGS sulfate and fraction as a function of time. Figure 6.60 (b) shows the uncertainty range on these estimates, calculated by taking plus or minus twice the total standard error  $E_{total}$ . While the best estimates of the NGS contribution is at times greater than the maximum possible (100 percent), the uncertainty bars span physically possible values.

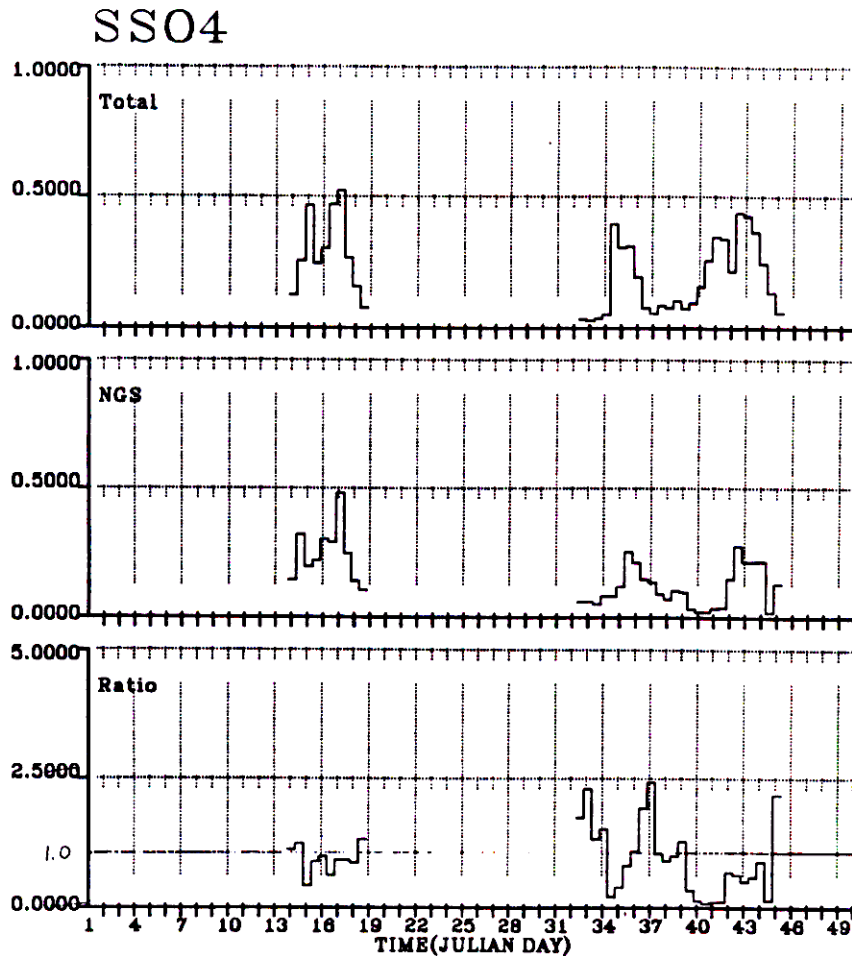


Figure 6.60: a: Time histories of the best estimates of ambient sulfate sulfur ( $\mu\text{g}/\text{m}^3$ ), sulfate sulfur due to NGS ( $\mu\text{g}/\text{m}^3$ ), and the ratio of NGS/ambient at Hopi Point.

Tables 6.42 and 6.43 and Figures 6.61 and 6.62 show similar results for  $\text{SO}_2$  and total sulfur (the sum of  $\text{SO}_2$  and sulfate).

Table 6.41: Time history of measured  $SO_4$  ( $\mu g/m^3$ ), NGS  $SO_4$  ( $\mu g/m^3$ ) and fraction of ambient sulfate due to NGS based on DMB analysis for Hopi Point.

Julian Day	Total Measured $SO_4$			NGS Contribution to $SO_4$			Fraction Due to NGS		
	Ambient $SO_4$ Concent	Uncertainties due to K's	due to Measmt	NGS $SO_4$ Concent	Uncertainties due to K's	due to Measmt	Ratio	due to K's	due to Measmt
13.8	0.13	0.01	0.01	0.14	0.03	0.02	1.12	0.25	0.15
14.3	0.26	0.01	0.01	0.32	0.07	0.03	1.24	0.28	0.14
14.8	0.47	0.02	0.02	0.19	0.04	0.03	0.41	0.08	0.07
15.3	0.24	0.01	0.01	0.22	0.05	0.02	0.89	0.20	0.10
15.8	0.30	0.01	0.01	0.30	0.05	0.11	0.99	0.18	0.36
16.2	0.47	0.02	0.02	0.29	0.05	0.04	0.62	0.11	0.09
16.7	0.52	0.02	0.02	0.48	0.10	0.03	0.92	0.19	0.07
17.2	0.27	0.01	0.01	0.24	0.05	0.07	0.91	0.18	0.28
17.7	0.16	0.01	0.01	0.14	0.03	0.05	0.86	0.17	0.31
18.2	0.08	0.01	0.01	0.10	0.02	0.02	1.32	0.30	0.27
32.2	0.03	0.00	0.00	0.06	0.03	0.01	1.75	0.76	0.39
32.7	0.03	0.00	0.00	0.06	0.01	0.02	2.29	0.45	0.99
33.2	0.04	0.00	0.00	0.05	0.02	0.01	1.33	0.58	0.24
33.7	0.05	0.00	0.00	0.08	0.02	0.05	1.52	0.32	0.97
34.2	0.40	0.02	0.02	0.08	0.02	0.02	0.20	0.06	0.06
34.7	0.31	0.01	0.01	0.12	0.04	0.09	0.39	0.12	0.30
35.2	0.31	0.01	0.01	0.25	0.05	0.05	0.81	0.15	0.16
35.7	0.19	0.01	0.01	0.21	0.05	0.05	1.08	0.24	0.26
36.2	0.08	0.00	0.00	0.14	0.04	0.01	1.92	0.59	0.21
36.7	0.06	0.00	0.00	0.13	0.03	0.04	2.42	0.56	0.72
37.2	0.09	0.00	0.00	0.09	0.02	0.01	1.04	0.24	0.13
37.7	0.08	0.00	0.00	0.07	0.02	0.01	0.90	0.21	0.18
38.2	0.10	0.01	0.01	0.10	0.02	0.01	0.99	0.22	0.11
38.7	0.07	0.00	0.00	0.10	0.02	0.03	1.28	0.26	0.36
39.2	0.10	0.01	0.01	0.03	0.01	0.02	0.33	0.07	0.22
39.7	0.16	0.01	0.01	0.02	0.00	0.02	0.12	0.03	0.15
40.2	0.26	0.01	0.01	0.02	0.00	0.01	0.07	0.01	0.03
40.7	0.35	0.02	0.02	0.03	0.01	0.03	0.10	0.02	0.08
41.2	0.34	0.02	0.02	0.04	0.01	0.03	0.11	0.02	0.08
41.7	0.22	0.01	0.01	0.15	0.03	0.09	0.68	0.14	0.41
42.2	0.44	0.02	0.02	0.27	0.05	0.04	0.62	0.12	0.11
42.7	0.42	0.02	0.02	0.21	0.05	0.07	0.50	0.11	0.18
43.2	0.37	0.02	0.02	0.21	0.05	0.02	0.58	0.13	0.06
43.7	0.25	0.01	0.01	0.22	0.04	0.10	0.88	0.16	0.41
44.2	0.14	0.01	0.01	0.02	0.01	0.03	0.13	0.04	0.21
44.7	0.06	0.00	0.00	0.13	0.02	0.04	2.18	0.41	0.73

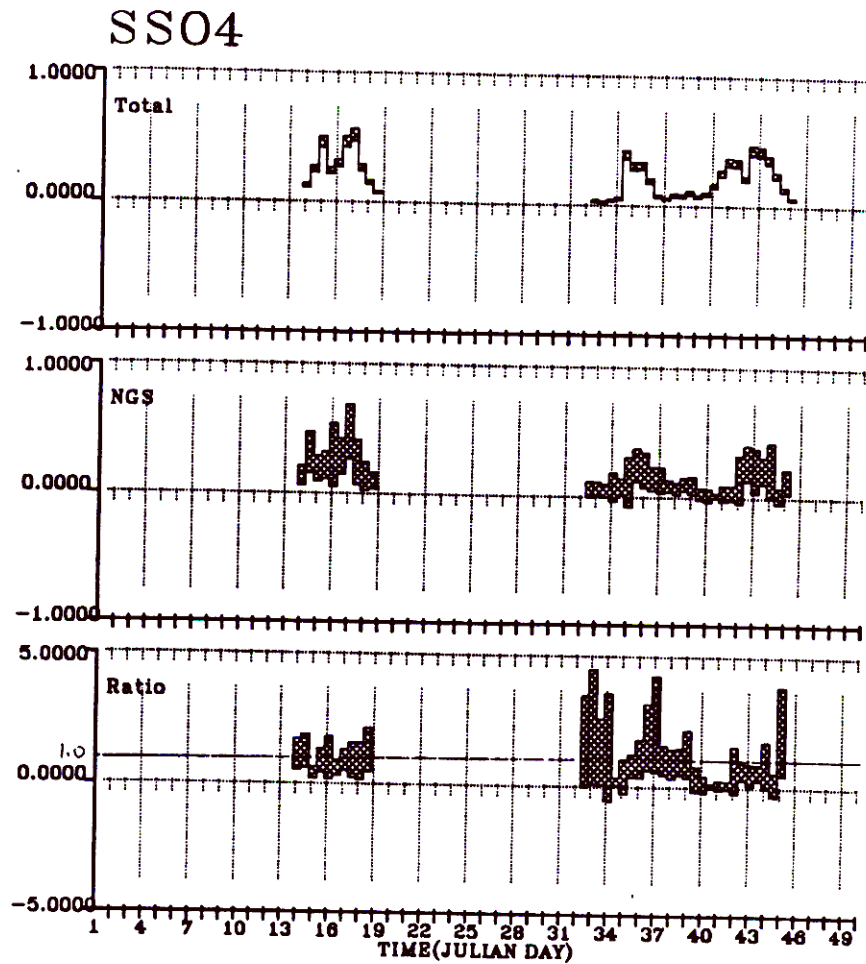


Figure 6.60: b: Time histories of the best estimates of ambient sulfate sulfur ( $\mu\text{g}/\text{m}^3$ ), sulfate sulfur due to NGS ( $\mu\text{g}/\text{m}^3$ ), and the ratio of NGS/ambient and their uncertainties at Hopi Point.

Table 6.42: Time history of measured  $SO_2$  ( $\mu g/m^3$ ), NGS  $SO_2$  ( $\mu g/m^3$ ) and fraction of ambient  $SO_2$  due to NGS based on DMB analysis for Hopi Point.

Julian Day	Total Measured $SO_2$			NGS Contribution to $SO_2$			Fraction Due to NGS		
	Ambient $SO_2$ Concent	Uncertainties due to K's	due to Measmt	NGS $SO_2$ Concent	Uncertainties due to K's	due to Measmt	Ratio	due to K's	due to Measmt
13.8	0.12	0.04	0.04	1.26	0.48	0.16	10.25	3.93	5.47
14.3	1.24	0.11	0.11	2.99	1.14	0.29	2.41	0.92	0.29
14.8	0.25	0.05	0.05	0.47	0.38	0.07	1.90	1.54	0.61
15.3	0.14	0.05	0.05	1.18	0.46	0.11	8.57	3.36	5.82
15.8	0.02	0.04	0.04	0.46	0.39	0.17	20.32	16.94	152.15
16.2	0.12	0.04	0.04	0.48	0.42	0.07	3.88	3.37	2.00
16.7	0.26	0.05	0.05	0.09	0.35	0.01	0.33	1.33	0.07
17.2	0.30	0.04	0.04	0.33	0.46	0.10	1.10	1.54	0.39
17.7	0.18	0.04	0.04	0.27	0.37	0.09	1.49	2.05	0.76
18.2	0.12	0.04	0.04	1.13	0.43	0.22	9.27	3.53	5.66
32.2	0.04	0.03	0.03	0.00	0.10	0.00	0.03	2.17	0.32
32.7	0.05	0.03	0.03	0.15	0.16	0.06	3.24	3.45	31.41
33.2	0.05	0.03	0.03	0.00	0.10	0.00	0.03	1.84	0.04
33.7	0.07	0.03	0.03	0.07	0.16	0.04	1.03	2.36	1.43
34.2	0.61	0.06	0.06	0.01	0.11	0.00	0.02	0.17	0.00
34.7	0.19	0.04	0.04	0.00	0.05	0.00	0.01	0.25	0.01
35.2	4.11	0.32	0.32	0.34	0.29	0.06	0.08	0.07	0.02
35.7	0.41	0.05	0.05	1.03	0.41	0.24	2.50	0.99	0.70
36.2	0.84	0.07	0.07	0.01	0.22	0.00	0.02	0.27	0.00
36.7	1.27	0.10	0.10	1.53	0.58	0.42	1.20	0.46	0.35
37.2	0.67	0.06	0.06	0.99	0.38	0.10	1.49	0.57	0.21
37.7	0.63	0.06	0.06	0.65	0.25	0.12	1.04	0.40	0.23
38.2	0.44	0.05	0.05	0.13	0.30	0.01	0.30	0.68	0.05
38.7	0.17	0.03	0.03	0.17	0.23	0.05	1.01	1.40	0.36
39.2	0.25	0.04	0.04	0.08	0.10	0.05	0.31	0.42	0.23
39.7	0.39	0.04	0.04	0.17	0.07	0.21	0.45	0.17	0.55
40.2	0.53	0.05	0.05	0.08	0.07	0.04	0.16	0.13	0.07
40.7	0.30	0.05	0.05	0.07	0.06	0.06	0.22	0.18	0.20
41.2	0.15	0.04	0.04	0.17	0.07	0.12	1.11	0.44	1.14
41.7	0.05	0.03	0.03	0.55	0.22	0.33	11.02	4.44	524.72
42.2	0.10	0.04	0.04	0.65	0.39	0.09	6.33	3.81	6.39
42.7	0.04	0.04	0.04	0.76	0.31	0.26	21.28	8.59	961.66
43.2	0.03	0.03	0.03	1.01	0.40	0.10	28.99	11.46	335.39
43.7	0.01	0.03	0.03	0.24	0.27	0.11	25.46	28.13	362.56
44.2	0.03	0.03	0.03	0.00	0.01	0.00	0.03	0.52	0.31
44.7	0.09	0.03	0.03	0.04	0.10	0.01	0.45	1.11	0.53

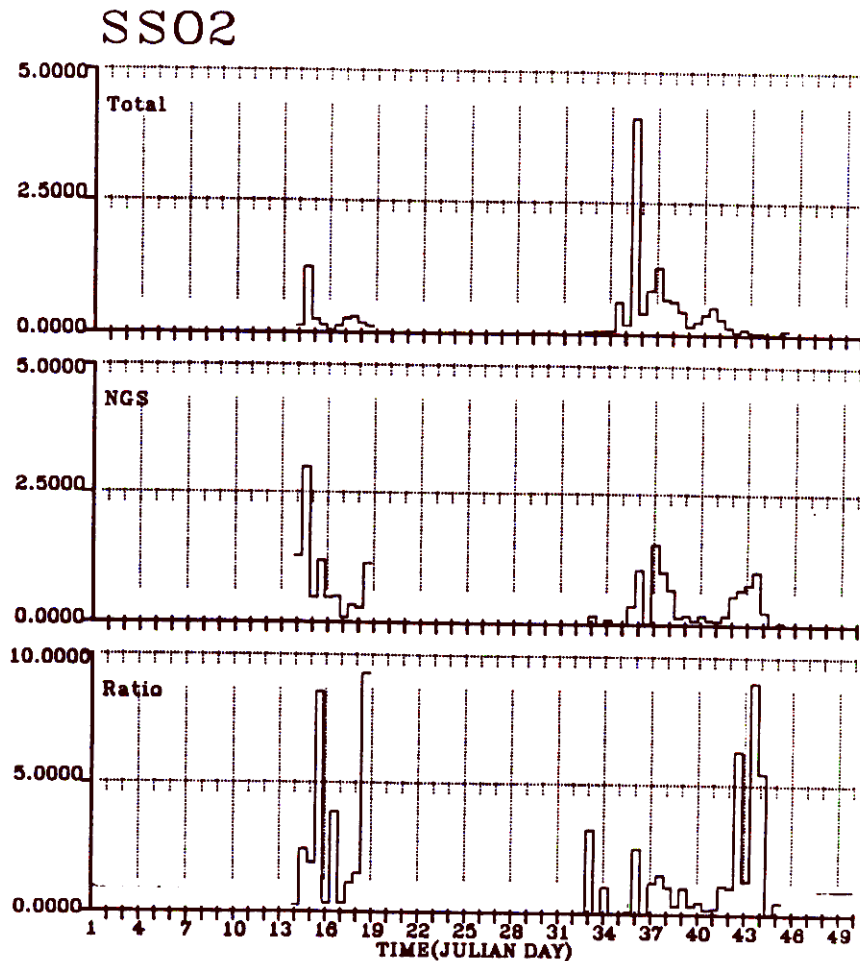


Figure 6.61: a. Time histories of the best estimates of ambient  $SO_2$  sulfur ( $\mu g/m^3$ ),  $SO_2$  sulfur due to NGS ( $\mu g/m^3$ ), and the ratio of NGS/ambient at Hopi Point.

The optimized DMB model was tested on both  $SO_2$  and sulfate concentrations at Hopi Point and at Page using different estimates of the NGS plume age. For Page, plume ages of 6 hours, 12 hours, the average of the minimum and maximum plume ages from Table 6.10 and the maximum NGS plume age from Table 6.10. For Hopi Point, the following four NGS plume ages were tested: the minimum estimated plume age from Table 6.10, the larger of 12 hours or the minimum NGS plume age (this was the set of ages used in the original optimization runs), the average of the minimum and maximum estimated NGS plume age, and the maximum plume age. Table 6.44 summarizes the average NGS contribution during WHITEX to  $SO_2$  and sulfate for each of these sites based on each of the assumed NGS plume ages tested.

The optimized DMB model shows that NGS contributes virtually all of the  $SO_2$  and sulfate measured in Page. If the NGS plume age in Page is assumed to be 6 hours, the NGS contribution to ambient sulfate is 59 percent. However, for this assumption the NGS contribution to ambient  $SO_2$  is 166 percent, a physical impossibility. Thus, the assumed 6-hour age in Page is most likely an underestimate. However, as we have seen in the prior DMB analysis, uncertainties are large.

Table 6.43: Time history of measured total sulfur ( $\mu\text{g}/\text{m}^3$ ), NGS total sulfur ( $\mu\text{g}/\text{m}^3$ ) and fraction of ambient total sulfur due to NGS based on DMB analysis for Hopi Point.

Julian Day	Total Measured <i>S</i>			NGS Contribution to <i>S</i>			Fraction Due to NGS		
	Ambient	Uncertainties		NGS	Uncertainties		Ratio	Uncertainties	
	<i>S</i> Concent	due to K's	due to Measmt	<i>S</i> Concent	due to K's	due to Measmt		due to K's	due to Measmt
13.8	0.25	0.04	0.04	1.40	0.47	0.18	5.63	1.90	1.28
14.3	1.50	0.11	0.11	3.31	1.12	0.31	2.21	0.75	0.24
14.8	0.71	0.05	0.05	0.66	0.38	0.11	0.93	0.53	0.17
15.3	0.38	0.05	0.05	1.39	0.44	0.13	3.65	1.16	0.66
15.8	0.33	0.04	0.04	0.76	0.38	0.28	2.34	1.18	0.93
16.2	0.59	0.04	0.04	0.77	0.42	0.11	1.30	0.71	0.20
16.7	0.78	0.05	0.05	0.57	0.37	0.04	0.72	0.47	0.06
17.2	0.57	0.04	0.04	0.57	0.47	0.17	1.01	0.83	0.32
17.7	0.34	0.04	0.04	0.40	0.37	0.14	1.20	1.11	0.47
18.2	0.20	0.04	0.04	1.23	0.42	0.24	6.19	2.12	1.90
32.2	0.08	0.03	0.03	0.06	0.10	0.01	0.78	1.26	0.76
32.7	0.07	0.03	0.03	0.22	0.17	0.09	2.90	2.23	2.52
33.2	0.09	0.03	0.03	0.05	0.10	0.01	0.57	1.10	0.38
33.7	0.12	0.03	0.03	0.15	0.16	0.10	1.24	1.36	0.89
34.2	1.01	0.06	0.06	0.09	0.11	0.02	0.09	0.11	0.02
34.7	0.50	0.04	0.04	0.12	0.06	0.09	0.24	0.11	0.19
35.2	4.42	0.33	0.33	0.59	0.29	0.10	0.13	0.06	0.03
35.7	0.61	0.05	0.05	1.24	0.39	0.29	2.05	0.64	0.53
36.2	0.91	0.07	0.07	0.16	0.23	0.01	0.17	0.26	0.02
36.7	1.33	0.10	0.10	1.66	0.57	0.46	1.25	0.43	0.36
37.2	0.75	0.06	0.06	1.08	0.37	0.11	1.43	0.49	0.19
37.7	0.71	0.06	0.06	0.72	0.24	0.13	1.02	0.35	0.22
38.2	0.55	0.05	0.05	0.24	0.31	0.02	0.43	0.56	0.06
38.7	0.24	0.03	0.03	0.26	0.24	0.07	1.10	0.98	0.35
39.2	0.34	0.04	0.04	0.11	0.11	0.07	0.31	0.31	0.22
39.7	0.55	0.04	0.04	0.19	0.07	0.24	0.35	0.12	0.43
40.2	0.79	0.06	0.06	0.10	0.07	0.04	0.13	0.09	0.06
40.7	0.65	0.05	0.05	0.10	0.06	0.08	0.16	0.08	0.13
41.2	0.49	0.04	0.04	0.20	0.06	0.14	0.42	0.13	0.30
41.7	0.27	0.04	0.04	0.69	0.21	0.41	2.60	0.78	1.67
42.2	0.54	0.04	0.04	0.93	0.39	0.14	1.71	0.71	0.29
42.7	0.46	0.04	0.04	0.98	0.29	0.33	2.12	0.63	0.79
43.2	0.40	0.04	0.04	1.22	0.38	0.12	3.05	0.96	0.41
43.7	0.25	0.04	0.04	0.46	0.27	0.21	1.79	1.06	0.90
44.2	0.16	0.03	0.03	0.02	0.01	0.03	0.12	0.09	0.21
44.7	0.15	0.03	0.03	0.17	0.10	0.05	1.14	0.70	0.50

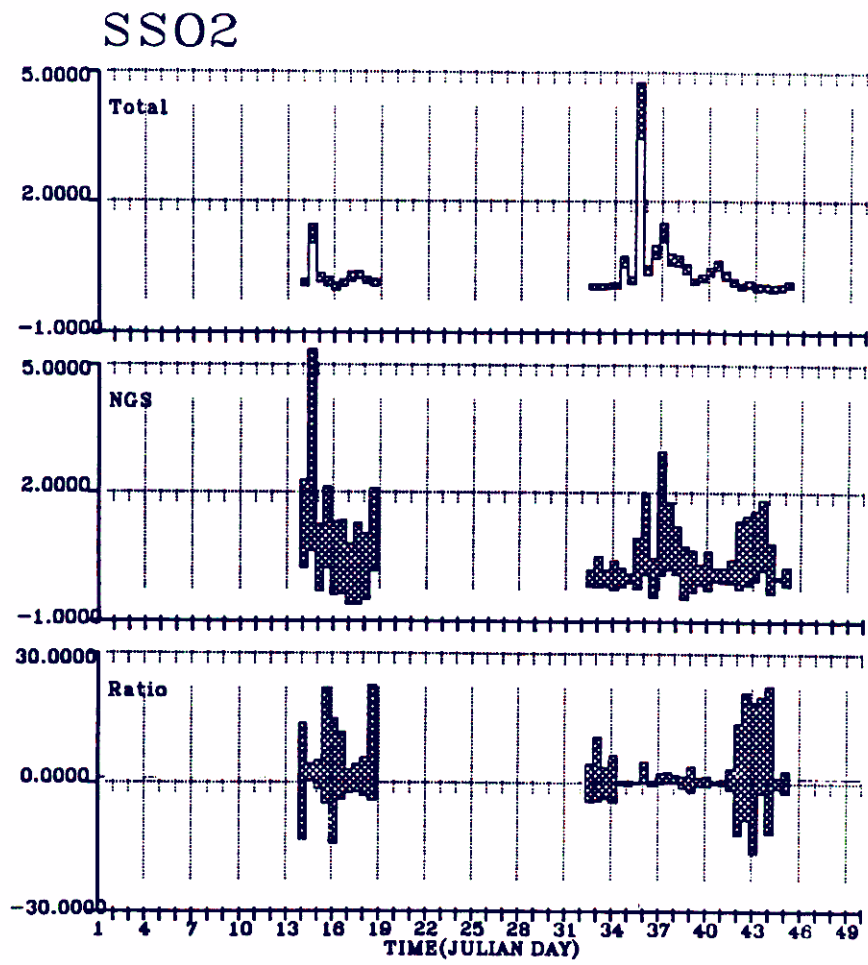


Figure 6.61: b. Time histories of the best estimates of ambient  $SO_2$  sulfur ( $\mu g/m^3$ ),  $SO_2$  sulfur due to NGS ( $\mu g/m^3$ ), and the ratio of NGS/ambient and their uncertainties at Hopi Point.

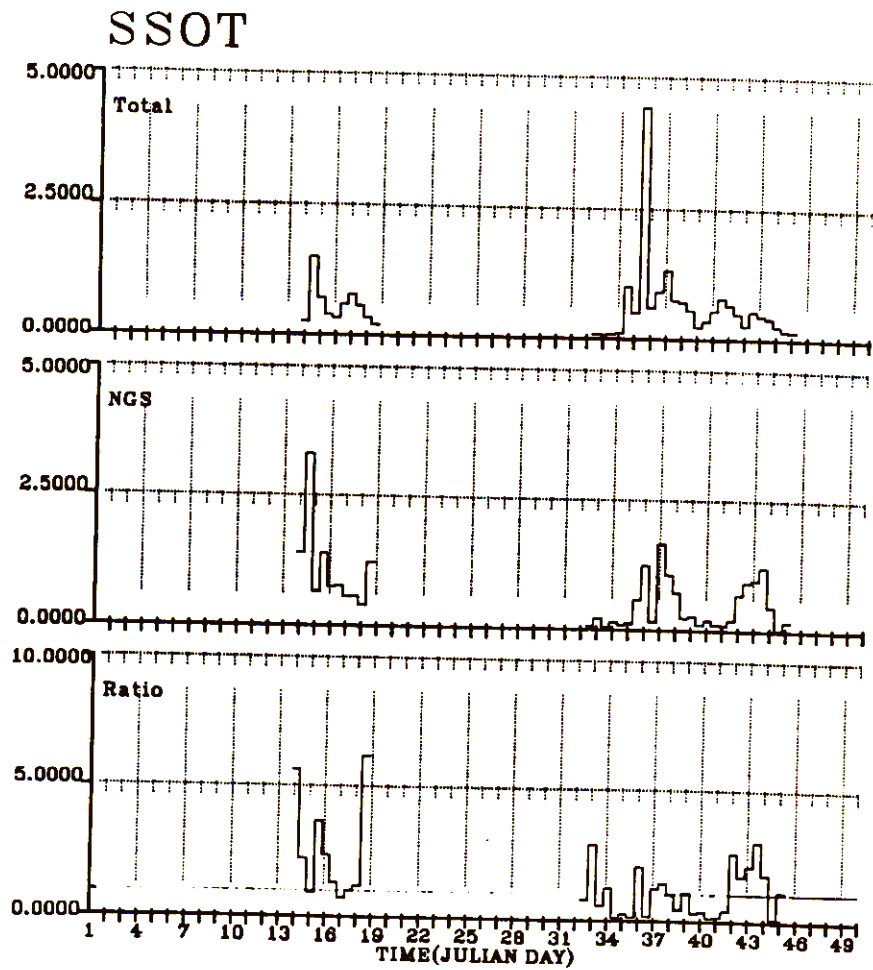


Figure 6.62: a. Time histories of the best estimates of ambient total sulfur ( $\mu\text{g}/\text{m}^3$ ), total sulfur due to NGS ( $\mu\text{g}/\text{m}^3$ ), and the ratio of NGS/ambient at Hopi Point.

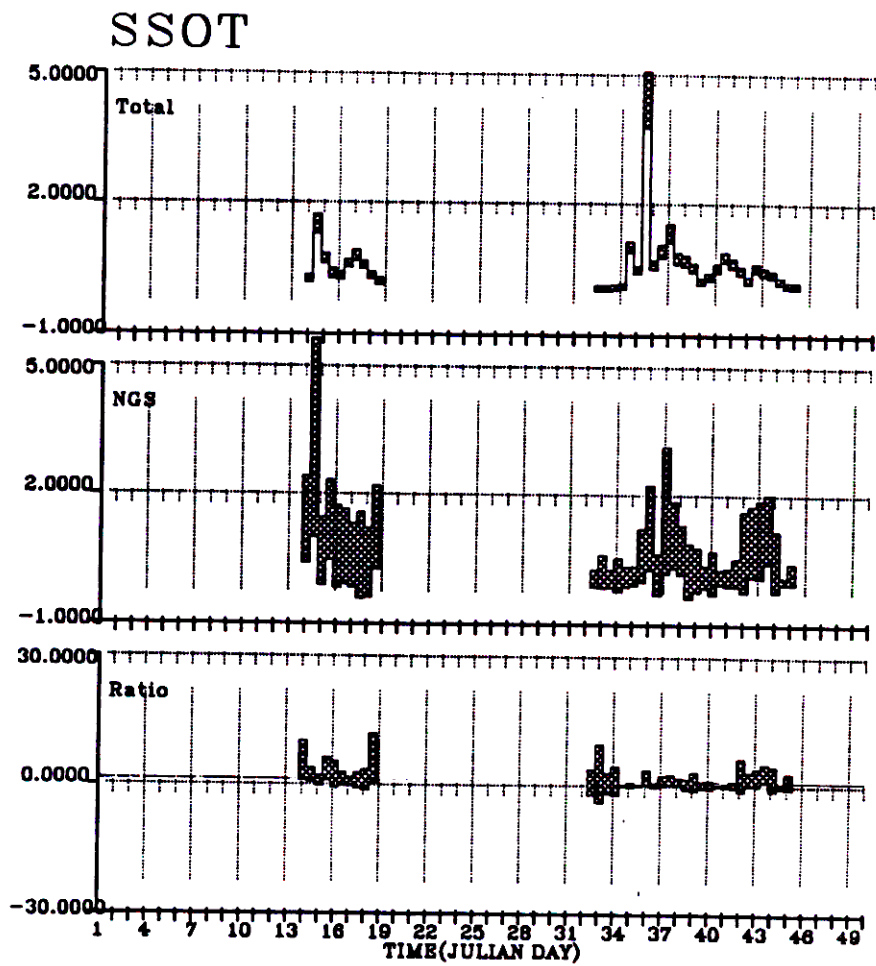


Figure 6.62: b. Time histories of the best estimates of ambient total sulfur ( $\mu\text{g}/\text{m}^3$ ), total sulfur due to NGS ( $\mu\text{g}/\text{m}^3$ ), and the ratio of NGS/ambient and their uncertainties at Hopi Point.

Table 6.44: Summary of DMB results: Overall average NGS contribution to  $SO_2$  and sulfate at Page, Arizona and Hopi Point as a function of estimated NGS plume age.

(a) Page

Assumption Regarding Plume Age	Average NGS Fraction	
	$SO_2$	$SO_4$
(1) 6 hours	1.659	0.591
(2) 12 hours	1.174	0.983
(3) Average of Minimum & Maximum Ages	1.056	1.019
(4) Maximum Plume Age	0.817	1.099

(b) Hopi Point

Assumption Regarding Plume Age	Average NGS Fraction	
	$SO_2$	$SO_4$
(1) Minimum Plume Age	1.553	0.602
(2) Larger of 12 hours or Minimum Age	1.231	0.682
(3) Average of Minimum & Maximum Ages	0.829	0.731
(4) Maximum Plume Age	0.645	0.727

Using the three larger values of NGS plume age, we find that the average NGS contribution to both  $SO_2$  and sulfate is not significantly different from 1.0 (100 percent).

For Hopi Point, the average NGS contribution to ambient sulfate is not particularly sensitive to the assumptions made regarding plume age. The NGS sulfate fraction varies from 60 to 73 percent over the range of assumed NGS plume ages. However, only the higher two of the NGS plume ages tested yield NGS  $SO_2$  contributions that are physically meaningful (i.e., <100%). For the average of the minimum and maximum NGS plume ages from Table 6.10, The DMB yields an average NGS contribution to  $SO_2$  at Hopi Point of 83 percent.

Figures 6.63, 6.64, and 6.65 show the time histories of the DMB-calculated NGS contributions to sulfate,  $SO_2$ , and total sulfur in Page, based on an assumed 12-hour plume age. Table 6.44 summarizes the DMB results for Page and Hopi Point.

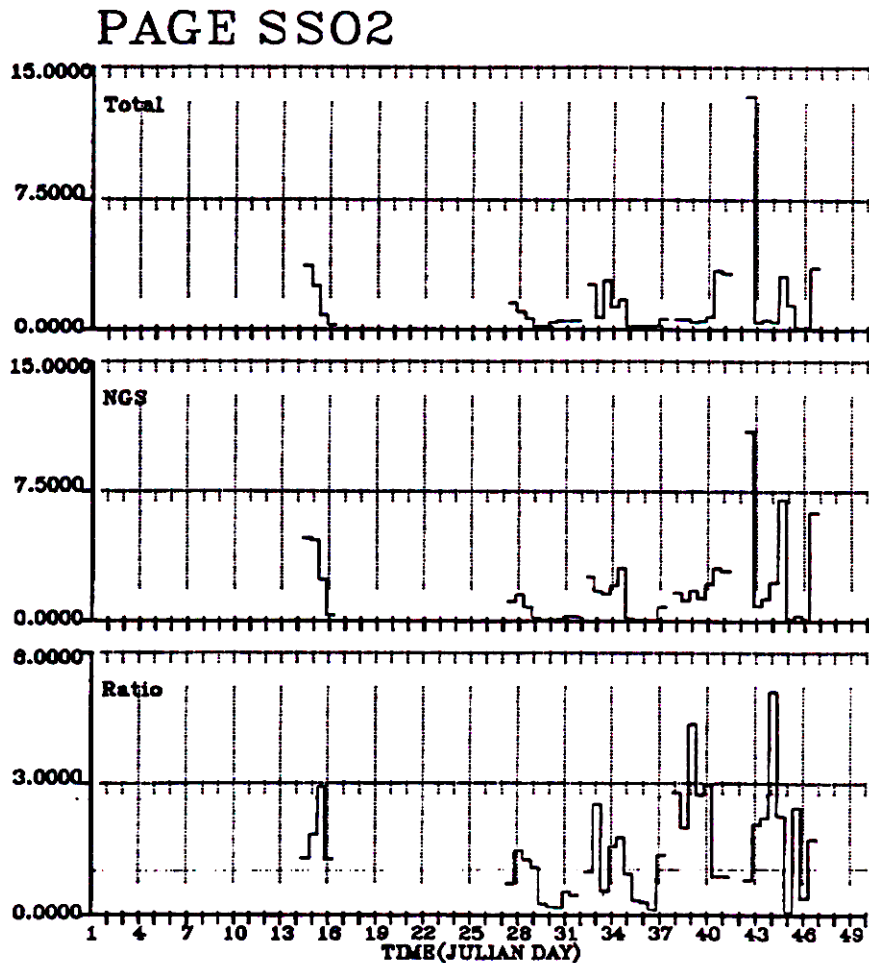


Figure 6.63: Time histories of the best estimates of ambient  $SO_2$  sulfur ( $\mu g/m^3$ ),  $SO_2$  sulfur due to NGS ( $\mu g/m^3$ ), and the ratio of NGS/ambient at Page.

PAGE SS04

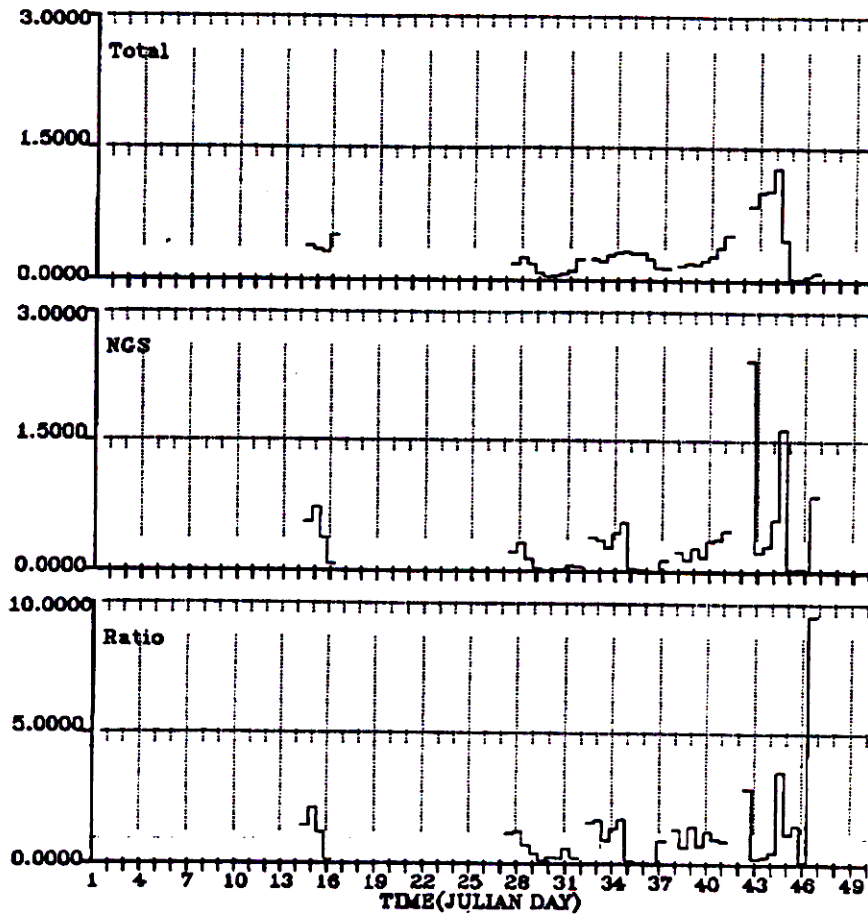


Figure 6.64: Time histories of the best estimates of ambient sulfate sulfur ( $\mu\text{g}/\text{m}^3$ ), sulfate sulfur due to NGS ( $\mu\text{g}/\text{m}^3$ ), and the ratio of NGS/ambient at Page.

# PAGE SSOT

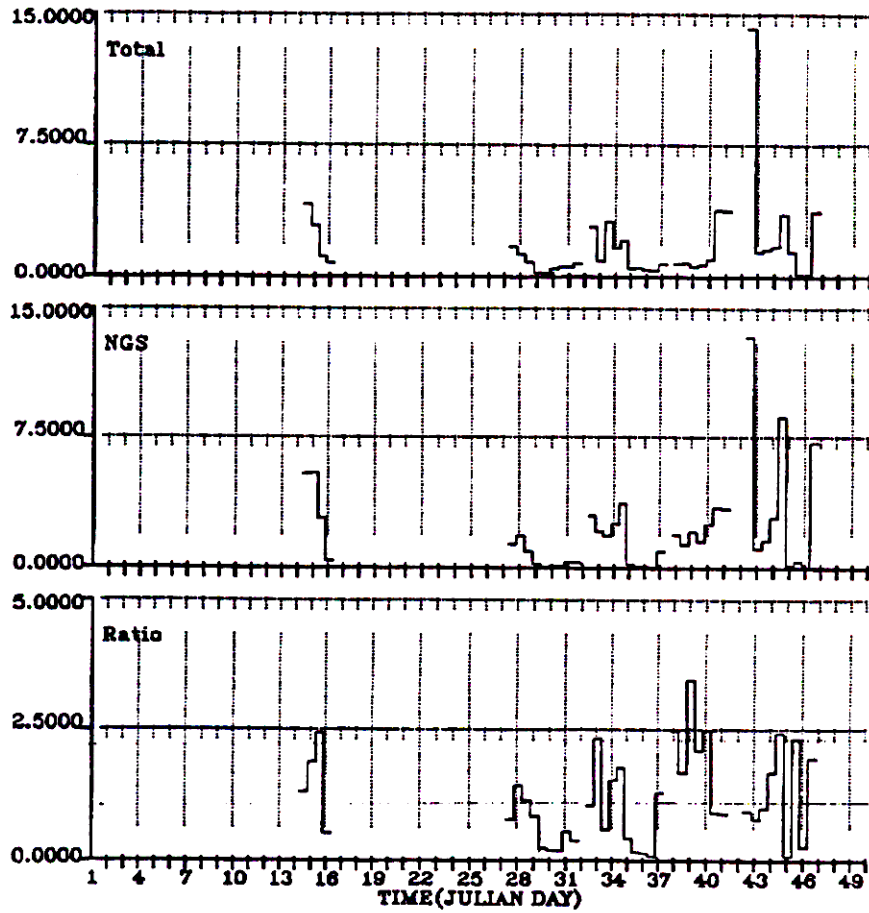


Figure 6.65: Time histories of the best estimates of ambient total sulfur ( $\mu\text{g}/\text{m}^3$ ), total sulfur due to NGS ( $\mu\text{g}/\text{m}^3$ ), and the ratio of NGS/ambient at Page.